Hindawi
International Journal of Aerospace Engineering
Volume 2021, Article ID 4163766, 11 pages
https://doi.org/10.1155/2021/4163766

*Research Article*

# Passive Sonar Multiple-Target Tracking with Nonlinear Doppler and Bearing Measurements Using Multiple Sensors

**Xiaohua Li**,[1,2] **Bo Lu**,[1,2] **Wasiq Ali**,[3] **Jun Su**,[3] **and Haiyan Jin**[1,2]

[1]*School of Computer Science and Engineering, Xi'an University of Technology, Xi'an 710048, China*
[2]*Shaanxi Key Laboratory for Network Computing and Security Technology, Xi'an 710048, China*
[3]*School of Marine Science and Technology, Northwestern Polytechnical University, Xi'an 710072, China*

Correspondence should be addressed to Xiaohua Li; lixiaohua@xaut.edu.cn

Received 22 June 2021; Accepted 21 September 2021; Published 11 October 2021

Academic Editor: Mahmut Reyhanoglu



The major advantage of the passive multiple-target tracking is that the sonars do not emit signals and thus they can remain covert, which will reduce the risk of being attacked. However, the nonlinearity of the passive Doppler and bearing measurements, the range unobservability problem, and the measurement to target data association uncertainty make the passive multiple-target tracking problem challenging. To deal with the target to measurement data association uncertainty problem from multiple sensors, this paper proposed a batch recursive extended Rauch-Tung-Striebel smoother- (RTSS-) based probabilistic multiple hypothesis tracker (PMHT) algorithm, which can effectively handle a large number of passive measurements including clutters. The recursive extended RTSS which consists of a forward filter and a backward smoothing is used to deal with the nonlinear Doppler and bearing measurements. The target range unobservability problem is avoided due to using multiple passive sensors. The simulation results show that the proposed algorithm works well in a passive multiple-target tracking system under dense clutter environment, and its computing cost is low.

## 1. Introduction

Passive multiple-target tracking has gained more and more attention in the fields of military and civilian, such as navigation, monitoring and early warning, and salvage [1–3]. How to discover targets timely and to track targets accurately becomes one of the hot topics. The aim of the multiple-target tracking is to estimate the expected targets' states, such as position, velocity, and acceleration, from the linear or nonlinear measurements [4–6]. The advantage of the passive target tracking is that the sonar can remain covert, which will reduce the risk of being attacked. The challenges for underwater passive multiple-target tracking include that the measurements are usually nonlinear, the target range may be unobservable, and the measurement to target data association is complex [5, 6].

In general, the passive measurements include bearing, Doppler, and bearing rate. So the passive multiple-target tracking is a typically nonlinear tracking problem [7–15]. One method to handle the nonlinear measurements is the pseudo linearization estimation (PLE) algorithm [16–18]. The other approach is the recursive nonlinear Bayesian filter and smoother, such as the extended Kalman filter (EKF) [19–22], the unscented Kalman filter (UKF) [23, 24], the cubature Kalman filter (CKF) [11, 12], and the particle filter (PF) [16]. EKF locally linearizes the targets' state and measurement equations using the first-order Taylor series expansion of the nonlinear transformations around the predicted target state. The merit of the EKF is that it is very easy to understand and apply to target tracking problem duo to its linear approximations to the nonlinear system or measurement function, and its computational cost is lower than that of other nonlinear filter, such as UKF and PF. The disadvantage of the EKF is that the tracking performance may be not good if the system model is seriously nonlinear or non-Gaussian.

The UKF uses a deterministic sampling method to capture targets' posterior distribution of mean and covariance based on the unscented transform. So the UKF has better tracking capability than the EKF to some extent, but its

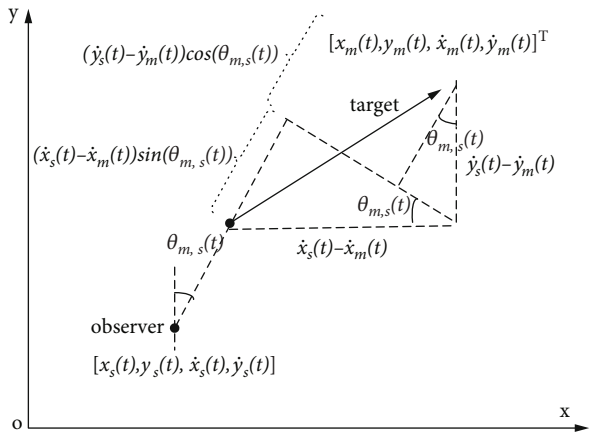


Figure 1: Multiple-target tracking scenario using Doppler and bearing measurement.

computational cost is larger than that of the EKF. The PF algorithm forms the Monte Carlo approximation to the solution of the Bayesian filter. It uses a set of particle samples to approximate the target distribution. The PF is used in the cases that the tracking system is highly nonlinear or non-Gaussian. The Bayesian filters only estimate the state of the targets from the history of measurements. On the contrary, the Bayesian smoother can use the forthcoming measurements to estimate the current state of targets. Corresponding to the Bayesian filter, the Bayesian smoother includes Rauch-Tung-Striebel smoother (RTSS), extended RTSS, unscented RTSS, and particle smoother [25].

The other challenge for passive sonar multiple-target tracking is the complexity and particularity of the underwater environment, which is characterized by many of false alarms caused by reverberation and multipath effect [3, 4]. Furthermore, the low target detection will cause tracking uncertainty in target location. All of those will cause a data association uncertainty problem. To handle the data association uncertainty problem, some algorithms are proposed, such as the multiple hypothesis trackers (MHT) [26], the joint PDA filter (JPDA) [27], the probabilistic MHT (PMHT) [28, 29], the random finite set framework-based probability hypothesis density (PHD) [30], the cardinalized PHD (CPHD) [31–33], and multi-Bernoulli filter (MBF). The MHT makes all the data association hypotheses probability optimal. The JPDA makes multiple hypotheses into a single hypothesis and performs the Kalman update with composite measurements. The PMHT is based on the expectation maximization (EM), which optimizes the multiple-target states' maximum a posteriori (MAP) estimation [34–36]. Different from the data association algorithms, the PHD, CPHD, and MBF are based on the random finite set theory, which makes all the measurements a measurement set and all the targets a target set.

The information entropy theories are also used to estimate the target states. The fuzzy $c$-means clustering method based on maximum information entropy and the probabilistic data association filter (PDA) is proposed in [37], which uses a value optimized by the maximum information entropy to represent the measurement to target association probability. The multiple-target tracking problem is also solved by the maximum entropy intuitionistic fuzzy data association [38], cross entropy [39], maximum fuzzy entropy-based Gaussian clustering algorithm [40], entropy distribution and game theory based on the probability hypothesis density (PHD) method [41], maximum entropy fuzzy based on the fire-fly and PF [42], and the distributed cross entropy-based $\delta$-generalized labelled multi-Bernoulli filter [43].

Table 1: Batch recursive multiple-sensor PMHT.

| |
|---|
| 1. Initialization |
| Initialize the target states $\hat{\mathbf{x}}_m(0 \mid 0)$ and $\mathbf{P}_m(0 \mid 0)$. |
| 2. Set the EM iteration $n = 1$. Calculate the target state prediction $\mathbf{x}_m^{(n)}(t \mid t-1)$ and state covariance $\mathbf{P}_m^{(n)}(t \mid t-1)$. |
| 3. Calculate the posterior association probabilities $w_{m,r}^{(n)}(t,s)$ in (15). |
| 4. Evaluate the synthetic Doppler and bearing measurements $\tilde{\mathbf{z}}_{m,s}(t)$ and covariance $\tilde{\mathbf{R}}_{m,s}(t)$ in (20) and (21). |
| 5. Evaluate the innovation covariance and filter gain for each target and passive sensor. |
| 6. Update the target state $\mathbf{x}_m^{(n)}(t \mid t)$ and state prediction covariance $\mathbf{P}_m^{(n)}(t \mid t)$ for each target $m$ according to the extended RTSS. |
| 7. Forward $n = n + 1$. Repeat the EM algorithm of steps 3 to 6 until the iteration convergent. |

As for the target range unobservability problem, the target range is observable from bearing and Doppler measurements if and only if the bearings are not constant [44, 45]. So in order to avoid the range unobservability problem, this paper uses multiple passive sensors to track targets. In addition, the target tracking accuracy of using multiple sensors is better than that of the single sensor generally.

The most commonly used passive measurement is bearing. In this paper, in order to improve the multiple targets' range observability and tracking performance, we introduce the nonlinear Doppler measurement and use multiple sensors. The extended RTSS method is used to deal with the nonlinear Doppler and bearing measurements. The batch recursive multiple-sensor PMHT algorithm is used to handle the measurement to target data association complexity problem.

The remainder of this paper is as follows. The passive multiple-target tracking system model and measurement model are given in Section 2. Section 3 develops the multiple-sensor PMHT algorithm which is suitable for multiple-target tracking under dense clutter environment. The simulation result is given in Section 4. At last, a summary is given in Section 5.

## 2. System Model and Measurement Model

We consider the passive multiple-target tracking problem in a two-dimensional space.

*2.1. Tracking System Model.* Assume there are $M$ targets in the tracking space. The $m^{\text{th}}(m = 1, 2, \cdots, M)$ target's state is $\mathbf{x}_m(t) = (x_m(t), \dot{x}_m(t), y_m(t), \dot{y}_m(t))^T$, where $x_m(t)$ and $y_m(t)$ are the location of target $m$ in the $x$ and $y$ coordinate, respectively,

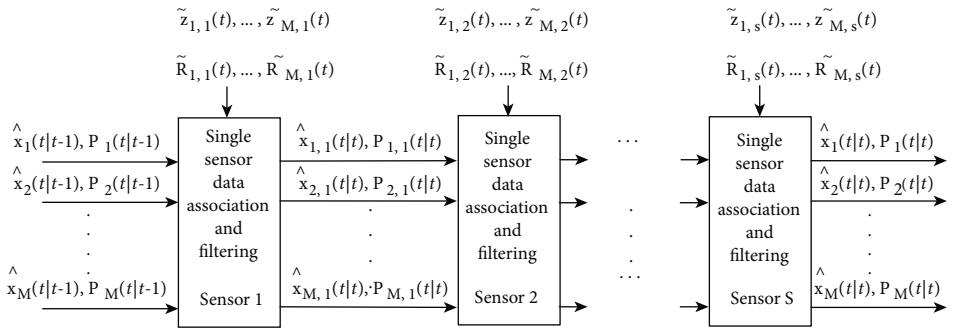


Figure 2: Sequential fusion implementation of multiple sensors.

Table 2: The five targets' initial position and velocity.

| Target | Position | Velocity |
|---|---|---|
| 1 | (800, 2000) m | (-22, -20) m/s |
| 2 | (1500, 1500) m | (20, -30) m/s |
| 3 | (500, -500) m | (23, 17) m/s |
| 4 | (0, 0) m | (-13, -27) m/s |
| 5 | (500, -1000) m | (13, -20) m/s |

and $\dot{x}_m(t)$ and $\dot{y}_m(t)$ are the velocity of target $m$. Assume the tracking time is from $t = 1$ to $t = N$. The overview of the multiple-target tracking using Doppler and bearing measurements is shown in Figure 1.

Assume that all the targets move according to the following constant velocity (CV) model or constant acceleration (CA) model [46].

$$\mathbf{x}_m(t) = \mathbf{F}\mathbf{x}_m(t-1) + \mathbf{u}_m(t), \tag{1}$$

where $\mathbf{u}_m(t)$ is the system process noise which is assumed as Gaussian white noise. $\mathbf{F}$ is the system state transition matrix. For the CV and CA models, $\mathbf{F}$ is denoted as $\mathbf{F}_{\mathrm{CV}}$ and $\mathbf{F}_{\mathrm{CA}}$, respectively, and

$$\mathbf{F}_{\mathrm{CV}} = \begin{bmatrix} 1 & \Delta t & 0 & 0 \\ 0 & 1 & 0 & 0 \\ 0 & 0 & 1 & \Delta t \\ 0 & 0 & 0 & 1 \end{bmatrix}, \tag{2}$$

$$\mathbf{F}_{CA} = \begin{bmatrix} 1 & \Delta t & 0.5\Delta t^2 & 0 & 0 & 0 \\ 0 & 1 & \Delta t & 0 & 0 & 0 \\ 0 & 0 & 1 & 0 & 0 & 0 \\ 0 & 0 & 0 & 1 & \Delta t & 0.5\Delta t^2 \\ 0 & 0 & 0 & 0 & 1 & \Delta t \\ 0 & 0 & 0 & 0 & 0 & 1 \end{bmatrix}, \tag{3}$$

where $\Delta t$ is the sampling interval.

The process noise covariance matrices for the CV and CA models are denoted as $\boldsymbol{Q}_{\mathrm{CV}}$ and $\boldsymbol{Q}_{\mathrm{CA}}$, respectively, which are given by

$$\boldsymbol{Q}_{\mathrm{CV}} = \delta_p^2 \begin{bmatrix} \frac{\Delta t^4}{4} & \frac{\Delta t^2}{2} & 0 & 0 \\ \frac{\Delta t^2}{2} & \Delta t^2 & 0 & 0 \\ 0 & 0 & \frac{\Delta t^4}{4} & \frac{\Delta t^2}{2} \\ 0 & 0 & \frac{\Delta t^2}{2} & \Delta t^2 \end{bmatrix}, \tag{4}$$

$$\boldsymbol{Q}_{\mathrm{CA}} = \delta_p^2 \begin{bmatrix} \frac{\Delta t^5}{20} & \frac{\Delta t^4}{8} & \frac{\Delta t^3}{6} & 0 & 0 & 0 \\ \frac{\Delta t^4}{8} & \frac{\Delta t^3}{3} & \frac{\Delta t^2}{2} & 0 & 0 & 0 \\ \frac{\Delta t^3}{6} & \frac{\Delta t^2}{2} & \Delta t & 0 & 0 & 0 \\ 0 & 0 & 0 & \frac{\Delta t^5}{20} & \frac{\Delta t^4}{8} & \frac{\Delta t^3}{6} \\ 0 & 0 & 0 & \frac{\Delta t^4}{8} & \frac{\Delta t^3}{3} & \frac{\Delta t^2}{2} \\ 0 & 0 & 0 & \frac{\Delta t^3}{6} & \frac{\Delta t^2}{2} & \Delta t \end{bmatrix}, \tag{5}$$

where $\delta_p^2$ is the process noise intensity.

*2.2. Measurement Model for Multiple Sensors.* Assume there are $S$ passive sensors in the target tracking space, and the $s^{\mathrm{th}}$ sensor's states is $\mathbf{x}_s(t) = (x_s(t), \dot{x}_s(t), y_s(t), \dot{y}_s(t))^T$, in which $x_s(t)$ and $y_s(t)$ are the location of the sensor $s$ and $\dot{x}_s(t)$ and $\dot{y}_s(t)$ are the velocity of passive sensor $s$.

The Doppler and bearing measurements are nonlinear with respect to targets' states and sensors' states, which are given by

$$\mathbf{z}_{m,s}(t) = \mathbf{h}_{m,s}(t) + \mathbf{w}_{m,s}(t), \tag{6}$$

in which $\mathbf{w}_{m,s}(t)$ is the measurement noise with a covariance matrix $\mathbf{R}_{m,s}(t)$.

The Doppler and bearing measurement function $\mathbf{h}_{m,s}(t)$ is given by

$$\mathbf{h}_{m,s}(t) = \left[\left[1 - \frac{(\dot{x}_m(t) - \dot{x}_s(t))\sin\theta_{m,s}(t) + (\dot{y}_m(t) - \dot{y}_s(t))\cos\theta_{m,s}(t)}{c}\right] f_0 \arctan\left(\frac{x_m(t) - x_s(t)}{y_m(t) - y_s(t)}\right)\right], \tag{7}$$

where $c$ is the sound speed in water, $f_0$ is targets' radiation frequency, and $\theta_{m,s}(t)$ is bearing from target $m$ and sensor $s$.

## 3. Multiple-Sensor PMHT

*3.1. PMHT for Multiple Sensors.* The following notations are used in this section.

$S$ is the total number of passive observers.

$M$ is the total number of targets.

$n_t$ is the number of measurements.

$T$ is the total number of tracking time.

$\mathbf{X}(t) = \{\mathbf{x}_{m,s}(t)\}$ is the set of target states at time $t$.

$\mathbf{Z}(t) = \{\mathbf{z}_{m,s}(t)\}$ is the set of measurements at time $t$.

$\mathbf{K}(t) = \{k_{r,s}(t)\}$ is the set of measurement-target assignments at time $t$.

$\mathbf{X} = \{\mathbf{X}(t)\}$ is the set of the target state for time $1, 2, \cdots, T$.

$\mathbf{Z} = \{\mathbf{Z}(t)\}$ is the set of measurements for time $1, 2, \cdots, T$.

$\mathbf{K} = \{\mathbf{K}(t)\}$ is the set of measurement-target assignments for time $1, 2, \cdots, T$.

The PMHT is a Bayesian framework-based batch recursive algorithm, which obtains the maximum a posteriori estimation of the target states based on the expectation maximization (EM) method [47].

Let $k_{r,s}(t) = m$ indicate that measurement $r$ from sensor $s$ at time $t$ is associated with target $m$. Assume the measurement to target assignment is independent from each other.

Define the prior probability of the $r^{\text{th}}$ measurement from the $s^{\text{th}}$ sensor and $m^{\text{th}}$ target as

$$p(k_{r,s}(t) = m) = \pi_m(t). \tag{8}$$

The MAP estimate of $\mathbf{X}$ is

$$\hat{\mathbf{X}}_{\text{MAP}} = \arg \max_{\mathbf{X}} \mathrm{E}\{\log(p(\mathbf{X} \mid \mathbf{Z}))\}. \tag{9}$$

In order to calculate the MAP, define the following auxiliary function as

$$Q\left(\mathbf{X}^{(n+1)}; \mathbf{X}^{(n)}\right) = \int_{\mathbf{K}} \log\left(p\left(\mathbf{X}^{(n+1)}, \mathbf{K} \mid \mathbf{Z}\right)\right) \cdot p\left(\mathbf{K} \mid \mathbf{X}^{(n)}, \mathbf{Z}\right) d\mathbf{K}, \tag{10}$$

where $n$ is the number of EM iteration.

The goal is to maximize the auxiliary function over $\mathbf{X}^{(n+1)}$ using an initialized target state $\mathbf{X}^{(0)}$. In each EM iteration step, the goal of the PMHT is to solve the following equation.

$$\mathbf{X}^{(n+1)} = \arg \max_{\mathbf{X}^{(n+1)}} Q\left(\mathbf{X}^{(n+1)}; \mathbf{X}^{(n)}\right). \tag{11}$$

We have

$$p(\mathbf{X}, \mathbf{Z}) = \prod_{m=1}^{M} p(\mathbf{x}_m(1)) \prod_{t=2}^{\mathrm{T}} \prod_{m=1}^{M} p(\mathbf{x}_m(t) \mid \mathbf{x}_m(t-1)) \cdot \prod_{s=1}^{S} \prod_{t=1}^{\mathrm{T}} \prod_{r=1}^{n_t} \left[\sum_{p=1}^{P} \pi_p N\left\{\mathbf{z}_{r,s}(t); \hat{\mathbf{z}}_{m,s}(t), \mathbf{R}_{m,s}(t)\right\}\right], \tag{12}$$

$$p(\mathbf{K}, \mathbf{Z}, \mathbf{X}) = \prod_{m=1}^{M} p(\mathbf{x}_m(1)) \prod_{t=2}^{\mathrm{T}} \prod_{m=1}^{M} p(\mathbf{x}_m(t) \mid \mathbf{x}_m(t-1)) \cdot \prod_{s=1}^{S} \prod_{t=1}^{\mathrm{T}} \prod_{r=1}^{n_t} \pi_m N\left\{\mathbf{z}_{r,s}(t); \hat{\mathbf{z}}_{m,s}(t), \mathbf{R}_{m,s}(t)\right\}. \tag{13}$$

According to the conditional probabilistic theory,

$$p(\mathbf{K} \mid \mathbf{Z}, \mathbf{X}) = \frac{p(\mathbf{K}, \mathbf{Z}, \mathbf{X})}{p(\mathbf{X}, \mathbf{Z})} = \prod_{s=1}^{S} \prod_{t=1}^{N} \prod_{r=1}^{n_t} w_{m,r}^{(n)}(t, s). \tag{14}$$

From (12), (13), and (14), the posterior association probability is

$$w_{m,r}^{(n)}(t, s) \triangleq p(k_m(t) \mid \mathbf{x}_m(t), \mathbf{z}_{r,s}(t)) = \frac{\pi_m N\left\{\mathbf{z}_{r,s}(t); \hat{\mathbf{z}}_{m,s}(t), \mathbf{R}_{m,s}(t)\right\}}{\sum_{m=1}^{M} \pi_m N\left\{\mathbf{z}_{r,s}(t); \hat{\mathbf{z}}_{m,s}(t), \mathbf{R}_{m,s}(t)\right\}}, \tag{15}$$

in which

$$\hat{\mathbf{z}}_{m,s}(t) = h(\mathbf{x}_m(t), \mathbf{x}_s(t)). \tag{16}$$

According to the conditional probabilistic theory,

$$p(\mathbf{K}, \mathbf{X} \mid \mathbf{Z}) = \frac{p(\mathbf{K}, \mathbf{X}, \mathbf{Z})}{p(\mathbf{Z})}. \tag{17}$$

Substituting equation (17) into equation (10), the defined auxiliary function is calculated as

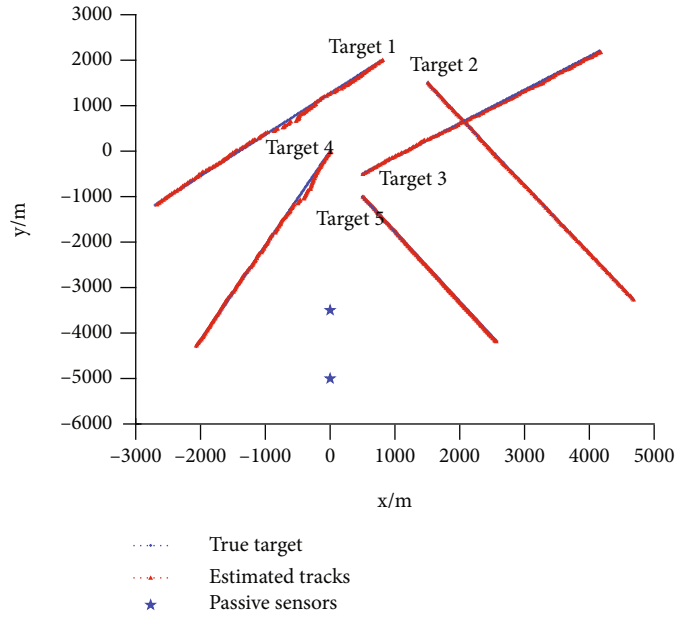


Figure 3: The tracking scenario of multiple targets, given two passive static sensors, true target trajectories, and estimated tracks.

$$Q\left(\mathbf{X}^{(n+1)};\mathbf{X}^{(n)}\right)=\int_{\mathbf{K}}\log\left(p\left(\mathbf{K},\mathbf{X}^{(n+1)},\mathbf{Z}\right)\right)\cdot p\left(\mathbf{K}\mid\mathbf{X}^{(n)},\mathbf{Z}\right)d\mathbf{K}-\log p(\mathbf{Z}). \tag{18}$$

The $\log p(\mathbf{Z})$ has no effect with regard to maximizing the auxiliary function $Q(\mathbf{X}^{(n+1)};\mathbf{X}^{(n)})$ in (18). So it can be removed from (18).

So the auxiliary function is given by

$$Q\left(\mathbf{X}^{(n+1)};\mathbf{X}^{(n)}\right)=\sum_{s=1}^{S}\sum_{t=1}^{\mathrm{T}}\sum_{r=1}^{n_t}\sum_{m=1}^{Q_{\Pi}=M}\log\pi_m w_{m,r}^{(n)}(t,s)+\underbrace{\log\left(\prod_{m=1}^{M}p\left(\mathbf{x}_m^{(n+1)}(1)\right)\prod_{t=2}^{\mathrm{T}}p\left(\mathbf{x}_m^{(n+1)}(t)\mid\mathbf{x}_m^{(n+1)}(t-1)\right)\right)+\sum_{s=1}^{S}\sum_{t=1}^{\mathrm{T}}\sum_{r=1}^{n_t}\sum_{m=1}^{M}\log p\left(\mathbf{z}_r(t)\mid\mathbf{x}_m^{(n)}(t)\right)w_{m,r}^{(n)}(t,s)}_{Q_{\mathbf{X}}}. \tag{19}$$

In order to maximize the auxiliary function, we compute its derivative and set the derivative to zero.

It turns out that the $\mathbf{X}^{(n+1)}$ is given by applying the extended RTSS method, in which the synthetic measurement $\tilde{\mathbf{z}}_{m,s}(t)$ and $\tilde{\mathbf{R}}_{m,s}(t)$ are calculated by

$$\tilde{\mathbf{z}}_{m,s}(t)=\frac{\sum_{r=1}^{n_t}w_{m,r}^{(n)}(t,s)\mathbf{z}_{r,s}(t)}{\sum_{r=1}^{n_t}w_{m,r}^{(n)}(t,s)}, \tag{20}$$

$$\tilde{\mathbf{R}}_{m,s}(t)\frac{\mathbf{R}_{m,s}(t)}{\sum_{r=1}^{n_t}w_{m,r}^{(n)}(t,s)}. \tag{21}$$

The implementation of the batch recursive multiple-sensor extended RTSS-based PMHT is depicted in Table 1.

*3.2. Recursive Extended RTSS.* The recursive extended RTSS is a linearized RTS smoother, which is based on analogous approximation to the EKF. It is a Gaussian approximation to the Bayesian smoother for the nonlinear target state and measurement model. The extended RTSS firstly performs the extended Kalman filter; then, a Kalman smoother is applied. That is, the extended RTSS consists of a forward filter and a backward smoother, which is summarized as follows:

Forward filter:

For $i=1,\cdots,T$,

Time update

$$\hat{\mathbf{x}}_m(t\mid t-1)=\mathbf{F}\hat{\mathbf{x}}_m(t-1\mid t-1), \tag{22}$$

$$\mathbf{P}_m(t\mid t-1)=\mathbf{F}\mathbf{P}_m(t-1\mid t-1)\mathbf{F}^{\mathrm{T}}+\mathbf{Q}_m(t). \tag{23}$$

Measurement update

$$\hat{\mathbf{x}}_m(t \mid t) = \hat{\mathbf{x}}_m(t \mid t-1) + \mathbf{G}_{m,s}(t)[\mathbf{z}_{m,s}(t) - \mathbf{h}_{m,s}(t \mid t-1)], \tag{24}$$

$$\mathbf{P}_m(t \mid t) = (\mathbf{I} - \mathbf{G}_{m,s}(t)\mathbf{H}_{m,s}(t)) \cdot \mathbf{P}_m(t \mid t-1) \cdot (\mathbf{I} - \mathbf{G}_{m,s}(t)\mathbf{H}_{m,s}(t))^{\mathrm{T}} + \mathbf{G}_{m,s}(t)\mathbf{R}_{m,s}(t)\mathbf{G}_{m,s}^{T}(t), \tag{25}$$

where the filter gain is

$$\mathbf{G}_{m,s}(t) = \mathbf{P}_m(t \mid t-1)\mathbf{H}_{m,s}^{T}(t) \cdot \left[\mathbf{H}_{m,s}(t)\mathbf{P}_m(t \mid t-1) \cdot \mathbf{H}_{m,s}^{T}(t) + \mathbf{R}_{m,s}(t)\right]^{-1}, \tag{26}$$

$$\mathbf{H}_{m,s}(t) = \left.\frac{\partial \mathbf{h}_{m,s}(t)}{\partial \mathbf{x}_m(t)}\right|_{\mathbf{x}_m(t)=\hat{\mathbf{x}}_m(t|t-1)}. \tag{27}$$

Backward smoothing:

For $i = T\text{-}1, \cdots, 1$,

$$\hat{\mathbf{x}}_m(t \mid \mathrm{T}) = \hat{\mathbf{x}}_m(t \mid t) + \mathbf{C}_m(t)[\hat{\mathbf{x}}_m(t+1 \mid \mathrm{T}) - \hat{\mathbf{x}}_m(t+1 \mid t)], \tag{28}$$

$$\mathbf{P}_m(t \mid \mathrm{T}) = \mathbf{P}_m(t \mid t) + \mathbf{C}_m(t)[\mathbf{P}_m(t+1 \mid \mathrm{T}) - \mathbf{P}_m(t+1 \mid t)]\mathbf{C}_m^{T}(t), \tag{29}$$

where

$$\mathbf{C}_m(t) = \mathbf{P}_m(t \mid t)\mathbf{F}^{T}\mathbf{P}_m^{-1}(t+1 \mid t). \tag{30}$$

For the Doppler and bearing measurement, the measurement Jacobian matrix is given by

$$\mathbf{H}_{m,s}(t) = \left[\frac{\partial \mathbf{h}_{m,s}(t)}{\partial x_m(t)} \; \frac{\partial \mathbf{h}_{m,s}(t)}{\partial \dot{x}_m(t)} \; \frac{\partial \mathbf{h}_{m,s}(t)}{\partial y_m(t)} \; \frac{\partial \mathbf{h}_{m,s}(t)}{\partial \dot{y}_m(t)}\right] = \begin{bmatrix} \dfrac{y_m(t) - y_s(t)}{r^2} & 0 & -\dfrac{x_m(t) - x_s(t)}{r^2} & 0 \\ 0 & \dfrac{-f_0[x_m(t) - x_s(t)]}{cr} & 0 & \dfrac{-f_0[y_m(t) - y_s(t)]}{cr} \end{bmatrix}, \tag{31}$$

where $r = \sqrt{(x_m(t) - x_s(t))^2 + (y_m(t) - y_s(t))^2}$.

*3.3. Data Fusion for Multiple Sensors.* For the tracking problem using multiple sensors, we need to fuse the target and measurement information from multiple sensors. The most used data fusion methods are parallel fusion and sequential fusion [48].

In this paper, we use the sequential data fusion for multiple sensors which updates the target state and covariance by each sensor sequentially. The multiple sensors deal with the measurements one after another with an intermediate target state and covariance at one time.

Let $\hat{\mathbf{x}}_{m,s}(t \mid t)$ and $\mathbf{P}_{m,s}(t \mid t)$ denote the target state estimation and corresponding covariance processed by the sensor $s$. The Doppler and bearing measurements from the first passive sensor are used to calculate the first intermediate target state $\hat{\mathbf{x}}_{m,1}^{(n)}(t \mid t)$ and covariance $\mathbf{P}_{m,1}^{(n)}(t \mid t)$ for each of the targets using a single sensor filter. Then, the measurements from the next passive sensor are used to update the intermediate target state and covariance as follows:

$$\hat{\mathbf{x}}_{m,s}(t \mid t) = \hat{\mathbf{x}}_{m,s-1}(t \mid t) + \mathbf{G}_{m,s}(t)[\mathbf{z}_{m,s}(t) - \mathbf{h}_{m,s}(t \mid t)], \tag{32}$$

$$\mathbf{P}_{m,s}(t \mid t) = (\mathbf{I} - \mathbf{G}_{m,s}(t)\mathbf{H}_{m,s}(t)) \cdot \mathbf{P}_{m,s-1}(t \mid t) \cdot (\mathbf{I} - \mathbf{G}_{m,s}(t)\mathbf{H}_{m,s}(t))^{\mathrm{T}} + \mathbf{G}_{m,s}(t)\mathbf{R}_{m,s}(t)\mathbf{G}_{m,s}^{T}(t), \tag{33}$$

where $\mathbf{G}_{m,s}(t)$ is the filter gain, and

$$\hat{\mathbf{x}}_{m,0}(t \mid t) = \hat{\mathbf{x}}_m(t \mid t-1), \mathbf{P}_{m,0}(t \mid t) = \mathbf{P}_m(t \mid t-1), \tag{34}$$

$$\hat{\mathbf{x}}_m(t \mid t) = \hat{\mathbf{x}}_{m,\mathrm{S}}(t \mid t), \mathbf{P}_m(t \mid t) = \mathbf{P}_{m,\mathrm{S}}(t \mid t). \tag{35}$$

The sequential fusion implementation of multiple sensors is shown in Figure 2.

## 4. Simulation

Assume the targets move in the two-dimensional space, and there are two static passive sensors. The two passive sensors deal with Doppler and measurements from targets and clutter. The two passive sensors located at (0, -3500) m and (0, -5500) m, respectively.

Assume that the clutter number is a Poisson distribution, and they are uniformly distributed in the Doppler and bearing measurement space. The average number of clutter in

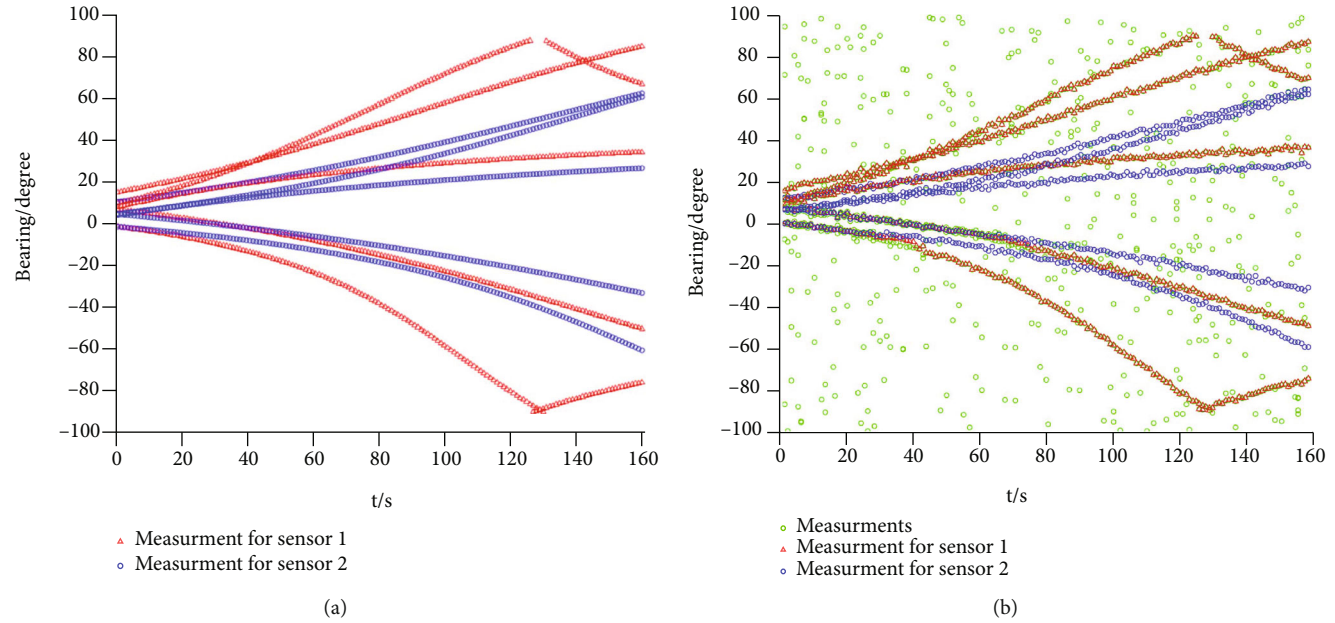


Figure 4: Bearing measurements for two static passive observers: (a) the true bearing measurements without clutter; (b) synthetic bearing measurements with clutter.

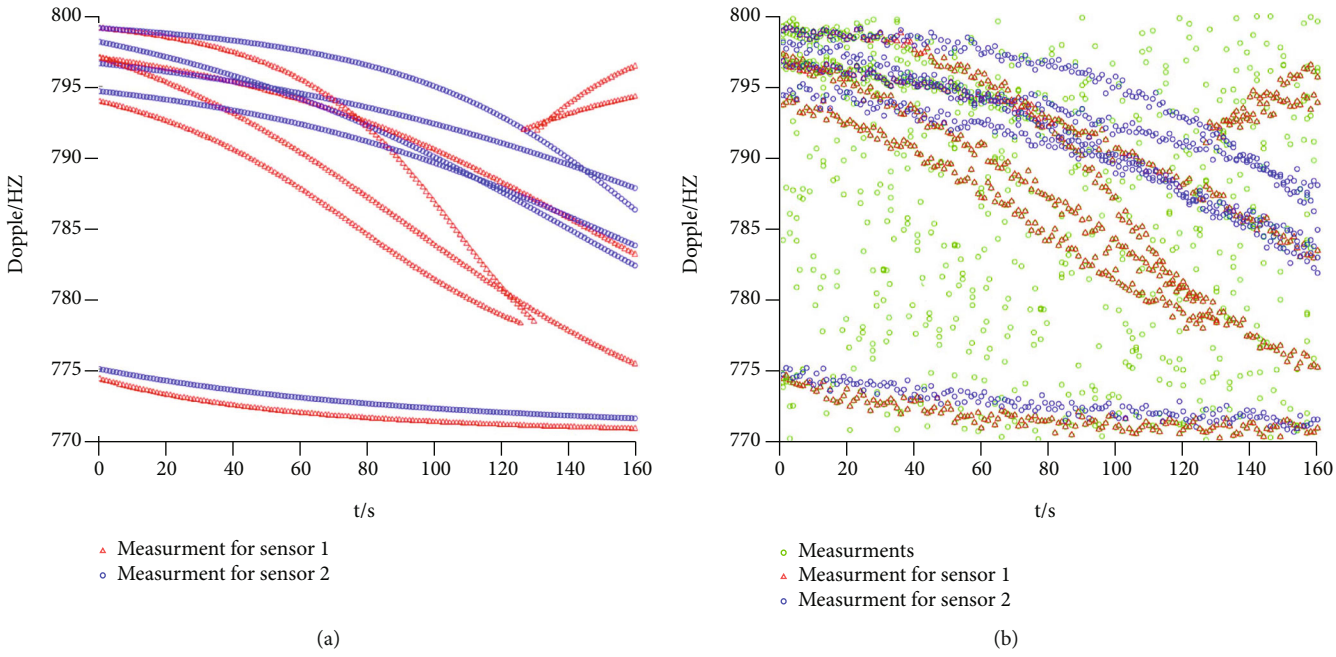


Figure 5: Doppler measurements for two static passive sensors: (a) the true Doppler measurements without clutter; (b) synthetic Doppler measurements with clutter.

each sampling scan is 20 in the Doppler and bearing measurements domain. The target detection probability is the same for all targets; here, we set it to 0.8. The tracking time is 160 s with a sampling interval 1 s. The Monte Carlo run is 200. The process noise intensity is 1 m. The Doppler measurement noise variance is 1 Hz, and the bearing noise variance is 0.8°.

*4.1. Case of the CV Model.* The five targets' initial position and velocity for the CV model are given in Table 2.

For the CV model, the simulated initial position $\mathbf{p}$ and velocity $\mathbf{v}$ are generated from the position $\mathbf{p}_0$ and velocity $\mathbf{v}_0$ of ground truth with an estimation error such that $\mathbf{p} = \mathbf{p}_0 + \mathbf{e}_1$ and $\mathbf{v} = \mathbf{v}_0 + \mathbf{e}_2$, where $\mathbf{e}_1 = 30$ m and $\mathbf{e}_2 = 2$ m/s.

The tracking scenario of true target trajectories and PMHT-estimated trajectories for the CV model is shown in Figure 3. The true Doppler and measurements for two static passive sensors without clutter and the PMHT synthetic Doppler and bearing measurements under dense clutter are given in Figures 4 and 5, respectively.

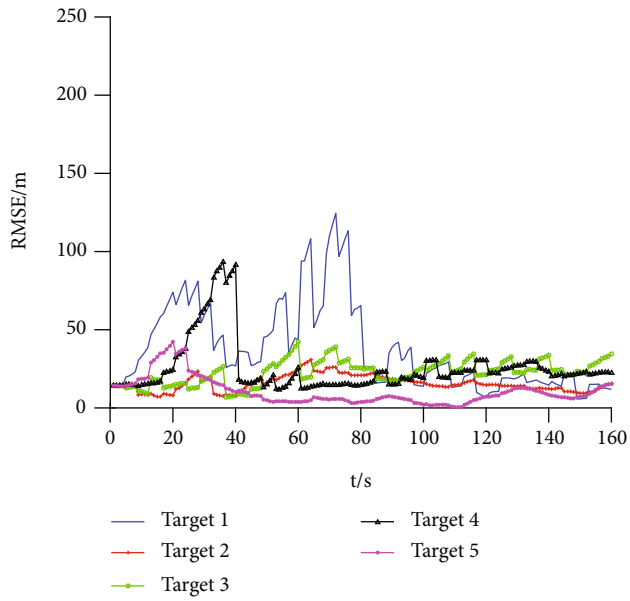


Figure 6: The position RMSE versus time scans of five targets.

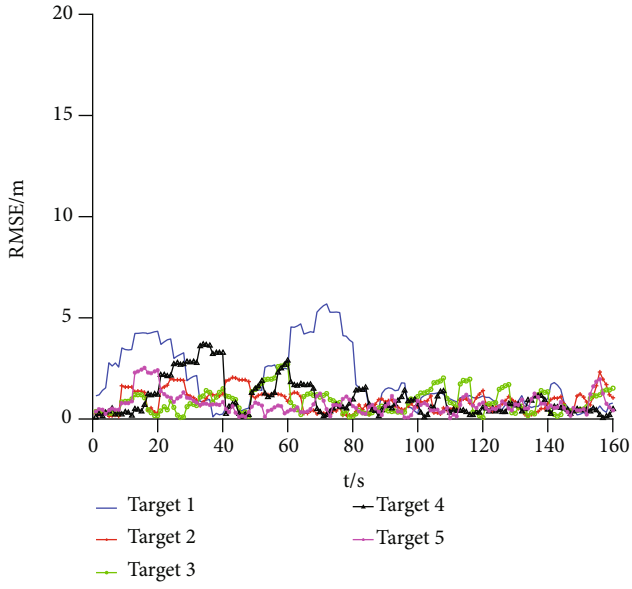


Figure 7: The velocity RMSE versus time scans of five targets.

In Figure 3, the extended RTSS-based PMHT algorithm can track all the five targets effectively; even if the target 1 and target 4 tracks are away from the true trajectory, the proposed algorithm can get the true target track after several time scans in the middle tracking time scan.

As seen in Figures 4 and 5, the density of Doppler and bearing measurement from clutter is high, and the synthetic Doppler and bearing measurement of the proposed algorithm broadly consists of the true Doppler and bearing measurements without clutter, which means that the proposed algorithm has good declutter ability.

The position and velocity RMSE of the five targets are given in Figures 6 and 7. Accordingly, the average position and velocity RMSE are shown in Tables 3 and 4. As shown

Table 3: The average position RMSE of five targets.

| Targets | 1 | 2 | 3 | 4 | 5 |
|---|---|---|---|---|---|
| RMSE (m) | 34.94 | 9.93 | 23.71 | 20.23 | 13.25 |

Table 4: The average velocity RMSE of five targets.

| Targets | 1 | 2 | 3 | 4 | 5 |
|---|---|---|---|---|---|
| RMSE (m/s) | 2.116 | 0.991 | 1.216 | 1.002 | 0.590 |

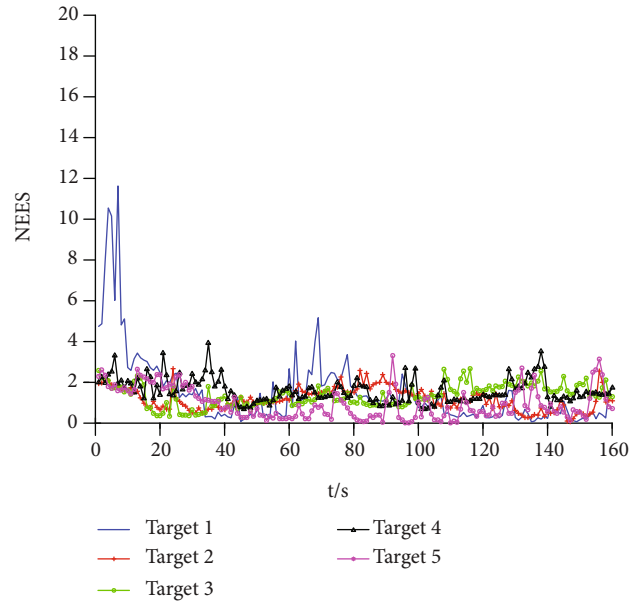


Figure 8: The average NEES versus time scans for five targets.

in Figures 6 and 7, the position RMSE and velocity RMSE for target 1 are increasing in the middle sampling scans, and as time goes on, the RMSE is decreased to a low lever, which is similar to other targets. This also can be seen from Tables 3 and 4. The average position and velocity RMSE is small which can meet the tracking accuracy requirement.

This paper uses the average normalized estimation error squared (ANEES) to evaluate the consistency of the proposed algorithm. For one target, the ANEES is defined as follows:

$$\mathrm{ANEES}(t) = \frac{1}{N_m}\sum_{i=1}^{N_m}\left(\mathbf{x}^i(t) - \hat{\mathbf{x}}^i(t)\right)^T \mathbf{P}^i(t)^{-1}\left(\mathbf{x}^i(t) - \hat{\mathbf{x}}^i(t)\right), \tag{36}$$

where $N_m$ is Monte Carlo runs, $\mathbf{x}^i(t)$ is the true target state, $\hat{\mathbf{x}}^i(t)$ is the estimated target state, and $\mathbf{P}^i(t)$ is the target state covariance.

The ANEES for fives targets is shown in Figure 8. As can be seen in Figure 8, the consistency of the proposed algorithm is good.

*4.2. Case of the CA Model.* The four targets' initial position, velocity, and acceleration for the CA model are given in Table 5.

Table 5: The five targets' initial position and velocity.

| Target | Position | Velocity | Acceleration |
|---|---|---|---|
| 1 | (800, 2000) m | (-22, -20) m/s | (0.3, 0) m/s$^2$ |
| 2 | (1500, 1500) m | (20, -30) m/s | (0, -0.3) m/s$^2$ |
| 3 | (500, -500) m | (23, 17) m/s | (0.4, 0.4) m/s$^2$ |
| 4 | (0, 0) m | (-13, -27) m/s | (0.1, 0.1) m/s$^2$ |

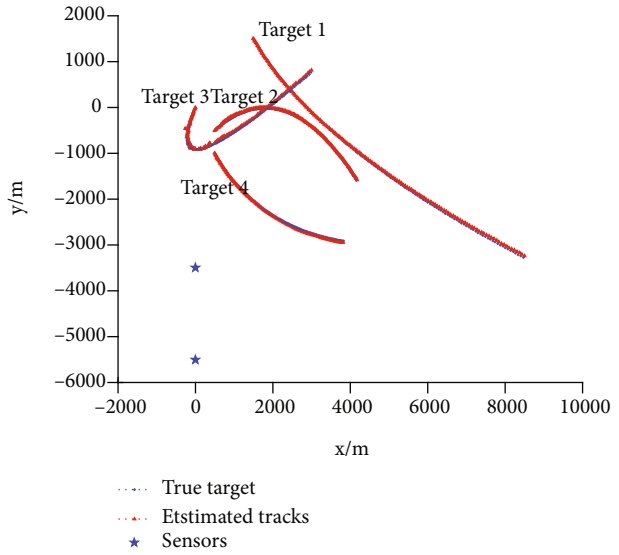


Figure 9: The tracking scenario of multiple targets, given two passive static sensors, CA model, true target trajectories, and estimated tracks.

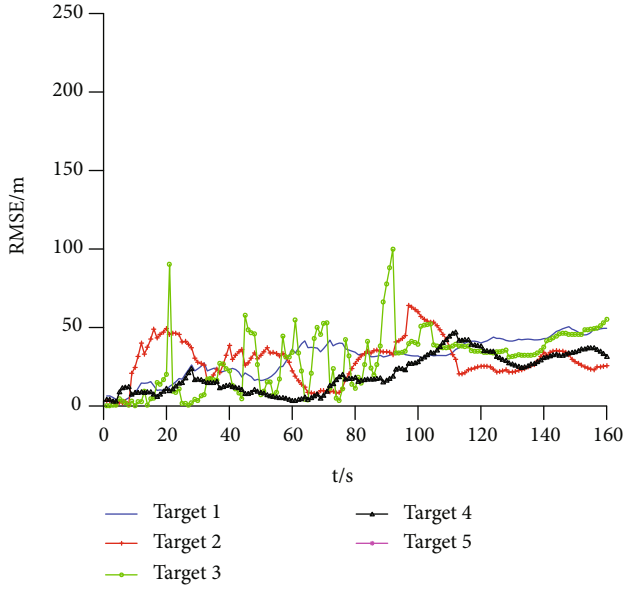


Figure 10: The position RMSE for four targets (CA model).

For the CA model, the simulated initial position $\mathbf{p}$, velocity $\mathbf{v}$, and acceleration $\mathbf{a}$ are generated from the position $\mathbf{p}_0$, velocity $\mathbf{v}_0$, and acceleration $\mathbf{a}_0$ of ground truth with an estimation error such that $\mathbf{p} = \mathbf{p}_0 + \mathbf{e}_1$, $\mathbf{v} = \mathbf{v}_0 + \mathbf{e}_2$, and $\mathbf{a} = \mathbf{a}_0 + \mathbf{e}_3$, where $\mathbf{e}_1 = 30$ m, $\mathbf{e}_2 = 2$ m/s, and $\mathbf{e}_3 = 0.5$ m/s$^2$.

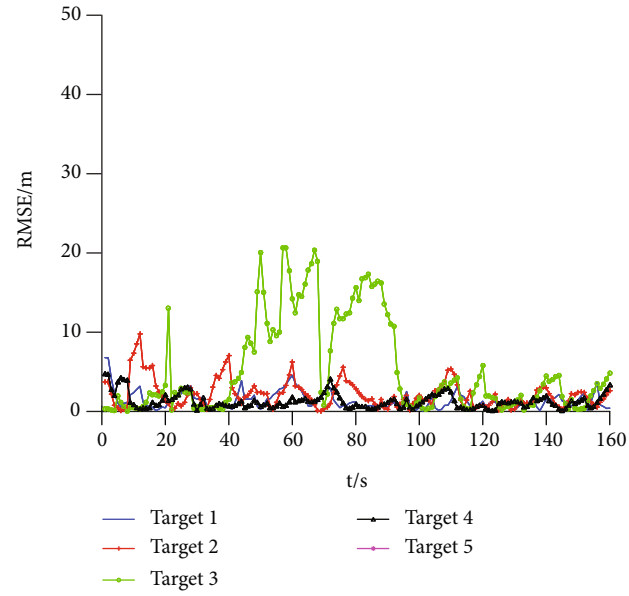


Figure 11: The velocity RMSE for four targets (CA model).

The tracking scenario of the CA model for target true trajectories and the estimated tracks is shown in Figure 9. Similar to the CV model, the estimated tracks are consistent with the true targets' trajectories.

The position RMSE and velocity RMSE for the CA model are shown in Figures 10 and 11. As shown in Figures 10 and 11, the position RMSE and velocity RMSE for target 3 are increasing in the middle sampling scans, and as time goes on, the RMSE is decreased to a low lever. The average position and velocity RMSE for the CA model is small which can meet the tracking accuracy requirement.

## 5. Conclusion

The major advantage of the passive sonars multiple-target tracking is that the sonars do not emit signals, and thus they can remain covert, which will reduce the risk of being attacked. But there are also challenges. Firstly, the Doppler and bearing measurements are nonlinear which makes the multiple-target tracking difficult. Secondly, the target states may be unobservable. Thirdly, the underwater environment is with dense clutter which will cause the measurement to target data association uncertainty problem. To deal with those problems, this paper proposed the extended RTSS-based batch PMHT method for multiple sensors and applied it to the passive multiple-sensor tracking system under dense clutter environment. This paper uses the extended RTSS algorithm to handle the nonlinear Doppler and bearing measurements. Multiple passive sonars are used to avoid the target state range unobservable problem. The multiple-sensor batch PMHT is used to deal with the data association uncertainty problem under dense clutter. The experiment results demonstrated that the proposed extended RTSS-based multiple-sensor PMHT algorithm can track multiple targets efficiently in the dense clutter environment, and the computing time is low.

## Data Availability

The simulation condition data used to support the findings of this study are included within the article.

## Conflicts of Interest

The authors declare that they have no conflicts of interest.

## Acknowledgments

This research was funded by the National Natural Science Foundation of China (61703333, 62076201, and U1934222), the Natural Science Basic Research Plan in Shaanxi Province of China (2019JQ-746, 2019-740), the Key Laboratory of Shaanxi Provincial Department of Education (20JS088), and the Science and Technology Project of Beilin District (GX2017).

## References

[1] M. S. Arulampalam, B. Ristic, N. Gordon, and T. Mansell, "Bearings-only tracking of maneuvering targets using particle filters," *EURASIP J. Appl. Signal Process.*, vol. 15, pp. 2351–2365, 2004.

[2] B. Ristic and M. S. Arulampalam, "Tracking a manoeuvring target using angle-only measurements: algorithms and performance," *Signal Processing*, vol. 83, no. 6, pp. 1223–1238, 2003.

[3] X. Chen, W. Li, Q. Lu, P. Willett, and Q. Zhang, "Underwater acoustic channel tracking by multi-Bernoulli filter," in *IEEE 2018 OCEANS*, pp. 1–8, Kobe, Japan, 2018.

[4] W. H. Foy, "Position-location solutions by Taylor series estimation," *IEEE Transactions on Aerospace and Electronic Systems*, vol. AES-12, no. 2, pp. 187–194, 1976.

[5] M. Ye, B. D. O. Anderson, and C. Yu, "Bearing-only measurement self-localization, velocity consensus and formation control," *IEEE Transactions on Aerospace and Electronic Systems*, vol. 53, no. 2, pp. 575–586, 2017.

[6] T. L. Song, "Observability of target tracking with bearings only measurements," *IEEE Transactions on Aerospace and Electronic Systems*, vol. 32, no. 4, pp. 1468–1472, 1996.

[7] I. Arasaratnam, S. Haykin, and R. Elliott, "Discrete-time nonlinear filtering algorithms using Gauss–Hermite quadrature," *Proceedings of the IEEE*, vol. 95, no. 5, pp. 953–977, 2007.

[8] R. Zanetti, "Recursive update filtering for nonlinear estimation," *IEEE Transactions on Automatic Control*, vol. 57, no. 6, pp. 1481–1490, 2012.

[9] R. Van Der Merwe and E. A. Wan, "The square-root unscented Kalman filter for state and parameter-estimation," in *Proceedings of the 2001 IEEE International Conference on Acoustics, Speech, and Signal Processing (ICASSP'01)*, pp. 3461–3464, Salt Lake City, UT, USA, 2001.

[10] B. Coraluppi, M. S. Arulampalam, and N. Gordon, *Beyond the Kalman Filter*, Artech House, Boston, MA, 2004.

[11] P. H. Leong, S. Arulampalam, T. A. Lamahewa, and T. D. Abhayapala, "A Gaussian-sum based cubature Kalman filter for bearings-only tracking," *IEEE Transactions on Aerospace and Electronic Systems*, vol. 49, no. 2, pp. 1161–1176, 2013.

[12] C. Hu, H. Lin, Z. Li, B. He, and G. Liu, "Kullback–Leibler divergence based distributed cubature Kalman filter and its application in cooperative space object tracking," *Entropy*, vol. 20, no. 2, p. 116, 2018.

[13] S. Konatowski, P. Kaniewski, and J. Matuszewski, "Comparison of estimation accuracy of EKF, UKF and PF filters," *Annual of Navigation*, vol. 23, no. 1, pp. 69–87, 2016.

[14] M. Arulampalam, S. Maskell, and N. Gordon, "A tutorial on particle filters for online nonlinear/non-Gaussian Bayesian tracking," *IEEE Transactions on Signal Processing*, vol. 50, no. 2, pp. 174–188, 2002.

[15] Z. M. Chen, Y. X. Qu, and B. Liu, "Improved multiple model target tracking algorithm based on particle filter," in *Proc. ImechE, Part G: J. Aerospace Engineering*, pp. 1–13, 2015.

[16] A. Miller and B. Miller, "Tracking of the UAV trajectory on the basis of bearing-only observations," in *Proc. 53rd IEEE Conf. Decision Control*, pp. 4178–4184, Los Angeles, CA, USA, 2014.

[17] A. Miller, "Developing algorithms of object motion control on the basis of Kalman filtering of bearing-only measurements," *Automation and Remote Control*, vol. 76, no. 6, pp. 1018–1035, 2015.

[18] A. Miller and B. Miller, "Underwater target tracking using bearing-only measurements," *Journal of Communications Technology and Electronics*, vol. 63, no. 6, pp. 643–649, 2018.

[19] Y. Bar-Shalom, X. Li, and T. Kirubarajan, *Estimation with Applications to Tracking and Navigation: Theory Algorithms and Software*, John Wiley & Sons, 2004.

[20] H. L. Van Trees and K. L. Bell, *Bayesian Bounds for Parameter Estimation and Nonlinear Filtering/Tracking*, Wiley, Hoboken, NJ, USA, 2007.

[21] A. Haug, *Bayesian Estimation and Tracking: A Practical Guide*, John Wiley & Sons, Hoboken, NJ, USA, 2012.

[22] P. Stano, Z. Lendek, J. Braaksma, R. Babuska, C. de Keizer, and A. J. den Dekker, "Parametric Bayesian filters for nonlinear stochastic dynamical systems: a survey," *IEEE Transactions on Systems, Man, and Cybernetics Part B, Cybernetics*, vol. 43, no. 6, pp. 1607–1624, 2013.

[23] R. Zhan and J. Wan, "Iterated unscented Kalman filter for passive target tracking," *IEEE Transactions on Aerospace and Electronic Systems*, vol. 43, no. 3, pp. 1155–1163, 2007.

[24] S. Särkkä, *Bayesian Filtering and Smoothing*, Cambridge Univ. Press, Cambridge, U.K., 2013.

[25] T. Lang and G. Hayes, "Evaluation of an MHT-enabled tracker with simulated multistatic sonar data," Proc. IEEE Oceans Conf, Aberdeen, Scotland, Jun, 2007.

[26] S. Coraluppi, C. Carthel, and M. Micheli, "DMHT-based undersea surveillance: insights from MSTWG analysis and recent sea-trial experimentation," in *Proc. 11th Int. Conf. Infor. Fusion*, pp. 1783–1790, 2008.

[27] W. Blanding, P. Willett, and Y. Bar-Shalom, "ML-PDA: advances and a new multitarget approach," *EURASIP Journal on Advances in Signal Processing*, vol. 2008, no. 1, 2007.

[28] M. Wieneke and W. Koch, "The PMHT algorithm: solutions for some of its problems," in *Proc. SPIE Conf.: signal data process. Small targets Conf*, vol. 6699, pp. 1–12, 2007.

[29] C. Rago, P. Willett, and R. Streit, "A comparison of the JPDAF and PMHT tracking algorithms," in *Proc Int. Conf. Acoustics, Speech, Signal Proc*, pp. 3571–3574, 1995.

[30] M. Beard and S. Arulampalam, "Performance of PHD and CPHD filtering versus JIPDA for bearings-only multitarget tracking," in *Proc. 15th Int. Conf. Infor. Fusion*, pp. 542–549, Singapore, 2012.

[31] O. Erdinc, P. Willett, and C. S. The, "Gaussian mixture cardinalized PHD tracker on MSTWG and SEABAR'07 datasets," in *Proc. 11th Int. Conf. Infor. Fusion*, pp. 1791–1798, Cologne, Germany, 2008.

[32] K. Pikora and F. Ehlers, "Analysis of the FKIE passive radar data set with GMPHD and GMCPHD," in *Proc. 16th Int. Conf. Infor. Fusion*, pp. 272–279, Istanbul, Turkey, 2013.

[33] R. Georgescu and P. Willett, *The GM-CPHD applied to the corrected TON-blind, adjusted SEABAR07 and Metron multistatic sonar datasets*, Proc. SPIE, 2010.

[34] C. Rago, P. Willett, and R. Streit, "Direct data fusion using the PMHT," *Proc. American Control Conf.*, vol. 3, pp. 1698–1702, 1995.

[35] S. Schoenecker, P. Willett, and Y. Bar-Shalom, "Maximum likelihood probabilistic multi-hypothesis tracker applied to multistatic sonar data sets," Proc. SPIE, 2011.

[36] Q. Lu, K. Domrese, P. Willett, Y. Bar-Shalom, and K. Pattipati, "A bootstrapped PHMT with feature measurements," *IEEE Transactions on Aerospace and Electronic Systems*, vol. 53, no. 5, pp. 2559–2571, 2017.

[37] X. Chen, Y. Li, J. Yu, and Y. Li, "Developing the fuzzy c-means clustering algorithm based on maximum entropy for multitarget tracking in a cluttered environment," *Journal of Applied Remote Sensing*, vol. 12, no. 1, article 016019, 2018.

[38] X. Zhan, X. Wang, and L. Li, "Online multi-object tracking via maximum entropy intuitionistic fuzzy data association," in *2018 14th IEEE International Conference on Signal Processing (ICSP)*, pp. 803–806, Beijing, China, 2018.

[39] M. Shozo and C. Chee, "Cross-entropy method for K-best dependent-target data association hypothesis selection," in *13th International Conference on Information Fusion*, Edinburgh, UK, 2010.

[40] X. Lian and A. Hamdulla, "A maximal fuzzy entropy based Gaussian clustering algorithm for tracking dim moving point targets in image sequences," in *2008 International Conference on Computer Science and Software Engineering*, pp. 54–57, Wuhan, China, 2008.

[41] X. Zhou, Y. Li, B. He, and T. Bai, "GM-PHD-based multitarget visual tracking using entropy distribution and game theory," *IEEE Transactions on Industrial Informatics*, vol. 10, no. 2, pp. 1064–1076, 2014.

[42] Y. Guo and J. Gong, "Group targets tracking using maximum entropy fuzzy based on fire-fly algorithm and particle filter," in *2020 7th International Forum on Electrical Engineering and Automation (IFEEA)*, pp. 937–942, Hefei, China, 2020.

[43] A. Saucan and P. Varshney, "Distributed cross-entropy $\delta$-GLMB filter for multi-sensor multi-target tracking," in *2018 21st International Conference on Information Fusion (FUSION)*, pp. 1559–1566, Cambridge, UK, 2018.

[44] K. Becker, "A general approach to TMA observability from angle and frequency measurements," *IEEE Transactions on Aerospace and Electronic Systems*, vol. 32, no. 1, pp. 487–494, 1996.

[45] C. Jauffret and D. Pillon, "Observability in passive target motion analysis," *IEEE Transactions on Aerospace and Electronic Systems*, vol. 32, no. 4, pp. 1290–1300, 1996.

[46] X. R. Li and V. P. Jilkov, "Survey of maneuvering target tracking . part I: dynamic models," *IEEE Transactions on Aerospace and Electronic Systems*, vol. 39, no. 4, pp. 1333–1364, 2003.

[47] D. Crouse, M. Guerriero, and P. Willet, "A critical look at the PMHT," *J. Adv. Infor. Fusion*, vol. 4, pp. 93–116, 2009.

[48] W. Saidani, Y. Morsly, and M. S. Djouadi, "Sequential versus parallel architecture for multiple sensors multiple target tracking," in *IEEE Conference on Human System Interactions*, pp. 904–908, Krakow, Poland, 2008.